

Rheology of Hydroxyethyl Guar Gum Derivatives

Romano Lapasin, Sabrina Pricl & Paolo Tracanelli

Istituto di Chimica Applicata e Industriale, Università di Trieste, Via Valerio 2, I-34127 Trieste, Italy

(Received 29 November 1989; revised version received 22 January 1990; accepted 31 January 1990)

ABSTRACT

The rheological properties of aqueous solutions of hydroxyethyl guar gum, a synthetic derivative of guar gum, have been studied under continuous and oscillatory shear flow conditions. Data obtained from both experimental techniques were satisfactorily fitted according to Cross-type models. The effect of polymer concentration, molecular weight and temperature on the rheological behavior of hydroxyethyl guar gum systems have been investigated and discussed in terms of rheological parameters like the zero-shear viscosity η_0 and the characteristic times λ and λ' .

INTRODUCTION

Galactomannans are water-soluble polysaccharides derived from the ground endosperm of a variety of plant seeds, where they act as reserve materials used during germination.

The chemical structure of galactomannans has been characterized as a linear (1 \rightarrow 4)-linked β -D-mannopyranosyl backbone, partially substituted at O-6 with α -D-galactopyranosyl side-groups (Dea & Morrison, 1975).

As extracted from various sources, these gums can differ widely in mannose to galactose ratio (M/G), distribution of side-groups along the main chain, molecular weight and molecular weight distribution.

Guar galactomannans are produced from the seeds of the *Cyanopsis tetragonoloba*, a native plant of India. Natural as well as chemically substituted guar gums are extensively used in the food, textile, printing and oil industries as thickening agents, mainly because they can impart

high viscosity to aqueous solutions even at low concentrations (Whistler, 1973).

The rheological properties of polymeric materials are related to polymer concentration, temperature and molecular parameters such as molecular weight, molecular weight distribution, etc. Hence, a better understanding of the relations between the rheological behavior and these parameters is important from the standpoints of both polymer preparation and processing.

A few recent papers have taken into consideration the rheological behavior of aqueous solutions of galactomannans (Sharman *et al.*, 1978; Naik, 1980; Morris *et al.*, 1981; Robinson *et al.*, 1982), but little work has been carried out to characterize fully water systems containing guar gum derivatives.

Hydroxyethyl guar gum (HEG), a synthetic derivative of guar gum, has been recently considered as a thickening agent in the formulation of textile printing pastes; however, the increasing use of these derivatives was not paralleled by a thorough rheological study.

The aim of this paper is a systematic investigation of the flow behavior of HEG aqueous solutions under steady and oscillatory flow conditions and an evaluation of the effects of polymer concentration, temperature and molecular parameters on the rheological properties of these systems.

This rheological characterization turns out to be a fundamental basis for the optimization in the formulation of industrial textile printing pastes, since the rheological properties of these materials are definitely determined by the polysaccharide matrix, as has been shown in a recent study (Lapasin *et al.*, 1988).

EXPERIMENTAL

Preparation and analysis of HEG derivatives

Commercial guar gum was partly hydrolysed with NaOH at high temperature to produce suitable molecular weight samples. Different molecular weights could be obtained by altering alkali concentration and/or reaction time.

The modification of guar gum was carried out by reaction with ethylene oxide in the presence of an alkaline catalyst.

Three HEG derivatives with different molecular weights but the same degree of substitution (DS) were prepared (HEG1, HEG2 and HEG3).

The molecular weight and molecular weight distribution were determined by gel-permeation chromatography (GPC) (Johnson & Porter,

1970) on a TSK PW column (Pharmacia LKB, Sweden), calibrated with fractionated pullulans (Poly-biòs-LBT, Italy) of known molecular weight.

The degree of substitution was determined by gas chromatography following the method suggested by Lee *et al.* (1983).

The results obtained are shown in Table 1.

Preparation of the samples

The effect of polymer concentration was studied on the HEG derivatives at 25°C. The concentrations (C_p , %w/w) considered were the following: HEG1: 1.00, 1.50, 2.32,* 3.10, 3.40, 4.00; HEG2: 1.00, 2.00, 4.88,* 6.00, 8.00; HEG3: 6.00, 8.00, 9.34,* 10.00, 12.00, 14.00. The asterisk indicates the concentration values employed in industrial formulation of textile printing pastes.

Apparatus and procedure

Experiments were performed on the systems prepared as reported in the previous section and left in the glass to rest overnight before use.

Continuous and dynamic tests were carried out with two different rotational rheometers.

Under continuous shear conditions, data in the lower shear rate range ($0.3\text{--}300\text{ s}^{-1}$) were obtained with a Haake Rotovisco RV100 measuring device CV100, mounted with a coaxial cylinder sensor system ZB15 (Couette type). During the tests, while the outer cup is driven, the inner cylinder is mechanically positioned and centered by an air bearing. Top and bottom surfaces are recessed to minimize end effects.

A Searle rheometer Haake RV20 measuring device M5-Osc, equipped with a cone-and-plate system (PK5-0.5) was employed to expand the shear rate range up to 6000 s^{-1} .

Stepwise procedures were applied for the analysis of the shear- and time-dependent properties in continuous shear flow.

TABLE 1
Weight-average Molecular Weight (\bar{M}_w), Molecular Weight Distribution (\bar{M}_w/\bar{M}_n) and Degree of Substitution (DS) for HEG Derivatives

	$\bar{M}_w \times 10^{-5}$	\bar{M}_w/\bar{M}_n	DS
HEG1	11.47	2.76	0.31
HEG2	3.63	2.91	0.29
HEG3	1.46	2.86	0.28

The multiple step procedure consists of a sequence of different shear rates $\dot{\gamma}$, each shear rate being kept constant until a steady value of the shear stress τ is attained. The analysis of the shear-dependent behavior can be properly based upon the steady values of τ obtained at different $\dot{\gamma}$ whereas the sequence of stress transients allows an evaluation of the extent of the time-dependent properties to be performed.

Oscillatory flow experiments were carried out in order to investigate the viscoelastic properties of these materials. All the measurements were performed with the Haake Rotovisco RV100 in a frequency range from 0.314 up to 7.536 rad/s at a constant strain of 2.4.

During the tests the outer cylinder was forced to oscillate sinusoidally at frequency ω , and the corresponding oscillation of the inner cylinder, proportional to the resultant torque, was recorded.

In the linear viscoelastic regime, the determination of the complex viscosity η^* (or the complex modulus G^*) and its viscous and elastic components η' and η'' (or G'' and G' , respectively) can be directly achieved by the analysis of the Lissajous figures obtained in a stress-strain plane.

The dynamic loss angle δ , defined as $\delta = \arctg G''/G'$, reflects the phase lag between stress and strain. As δ approaches $\pi/2$, the viscoelastic behavior reduces to that of a pure viscous liquid.

Calibration of the apparatus was performed by carrying out measurements on Newtonian fluids both in order to evaluate the response linearity of these systems under the selected operative conditions and to develop a standard procedure for the correction of the inertial effects.

Measurements were carried out at 20°C, 25°C and 30°C in order to evaluate the temperature effect on the rheological properties of HEG solutions.

RESULTS AND DISCUSSION

Continuous shear tests

Tests carried out under continuous shear conditions revealed that all the systems examined exhibit similar shear- and time-dependent properties.

As far as the time-dependent properties are concerned, no significant stress transient behavior has been observed for these systems by applying a stepwise procedure: each shear rate change implies an almost instantaneous variation of the shear stress to the corresponding equilibrium value.

The shear-dependent behavior of these solutions is markedly shear-thinning, and a typical logarithmic plot of viscosity η as a function of the applied shear rate $\dot{\gamma}$ is given in Fig. 1 for the HEG2 sample ($C_p = 4.88$).

At low $\dot{\gamma}$, the shear viscosity η approaches a constant value η_0 : the zero-shear-rate viscosity (upper Newtonian plateau). At higher $\dot{\gamma}$, η decreases with increasing $\dot{\gamma}$ and the flow curve exhibits a linear profile known as power-law region. The range of $\dot{\gamma}$ over which the transition from the upper Newtonian plateau to the power-law region occurs depends mainly on the molecular weight distribution of the sample: the broader the molecular weight distribution, the broader and more shifted to lower shear rates is the transition region (Graessley, 1974).

Finally, at a very high rate of shear, η may again become independent of $\dot{\gamma}$ and approaches another constant value, the so-called infinite-shear-rate viscosity η_∞ (lower Newtonian plateau). η_∞ cannot be generally evaluated since no experimental data can be easily obtained at very high shear rates.

The shear-thinning behavior of guar gum derivative solutions can be explained in terms of entanglement formation. Following Graessley (1974), the interpenetration of polymeric chains in concentrated solutions gives rise to a dynamic entangled network. In the upper Newtonian plateau, the disruption of entanglements by the imposed shear is dynamically balanced by the formation of new interactions between different chain segments; consequently, the extent of entanglement remains constant and no reduction in viscosity takes place. The

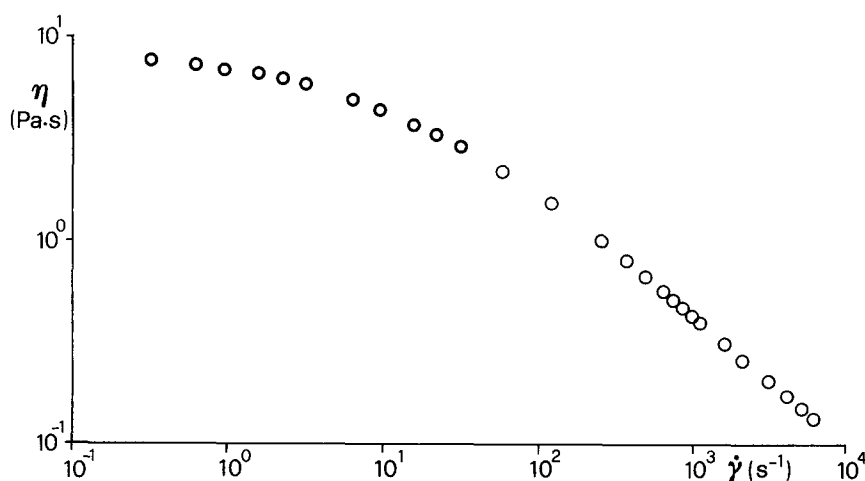


Fig. 1. Steady shear viscosity η versus shear rate $\dot{\gamma}$ for HEG2 ($C_p = 4.88\%$): ○, RV100-CV100 ZB15 data; ○, RV20-M50sc PK5-0.5 data.

onset of shear-thinning behavior corresponds to a different balance between the rate of externally imposed deformation and the rate of formation of new entanglements: thus the cross-links density of the network is depleted and η is reduced.

Simple rheological models that have been used in literature to describe the viscosity of many polymeric fluids that exhibit Newtonian behavior at low shear rates and power-law behavior at a high rate of deformation are the Carreau (1968) (eqn 1) and the Cross (1965) equations (eqn 2):

$$\eta = \eta_{\infty} + \frac{\eta_0 - \eta_{\infty}}{(1 + (\lambda\dot{\gamma})^2)^n} \quad (1)$$

$$\eta = \eta_{\infty} + \frac{\eta_0 - \eta_{\infty}}{1 + (\lambda\dot{\gamma})^n} \quad (2)$$

Since η_{∞} is usually negligible with respect to η_0 , it can be properly set equal to zero in such a way that these two equations are reduced to three adjustable parameter models: the zero-shear-rate viscosity η_0 , the characteristic time λ and an exponent n . The value of these parameters may be easily determined by fitting the experimental data.

It has to be pointed out here that, for the HEG2 system considered as an example, as well as for all the other systems studied in this work, the value of the n exponent of the Cross equation is very close to 2/3. It follows that for the handling of the experimental data the Cross model can be further reduced to a two-parameter version by definitely setting $n = 2/3$.

Since both the Carreau equation and the two-parameter Cross model can satisfactorily fit the viscosity rate of shear data, it can be more convenient to resort to the Cross equation for a comparison of the rheological properties of all the different systems examined.

Oscillatory flow tests

Under the experimental conditions considered, a Fourier analysis of the data has demonstrated that the dynamic response may be reduced to the fundamental harmonic.

In Fig. 2 the viscous component η' and the elastic component G' for the HEG2 system are plotted as a function of the frequency ω at an oscillation amplitude ϕ of 0.175 rad. The profiles of these curves are those typical of polymer concentrated solutions (Ferry, 1980).

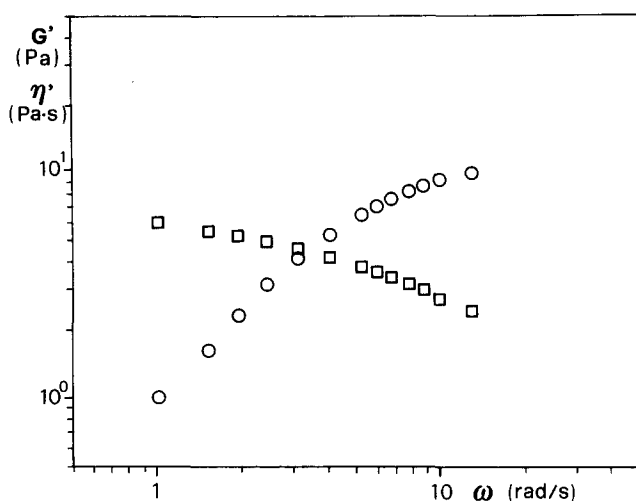


Fig. 2. Dynamic viscosity η' (\square) and storage modulus G' (\circ) as a function of oscillation frequency ω for HEG2 ($C_p = 4.88\%$).

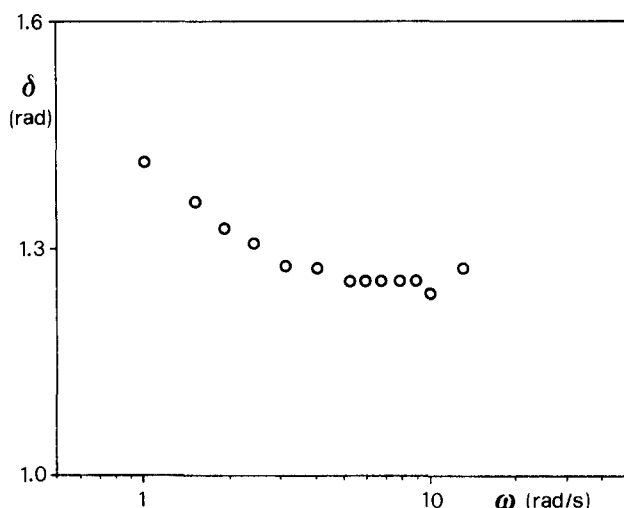


Fig. 3. Frequency dependence of the dynamic loss angle δ for HEG2 ($C_p = 4.88\%$).

The frequency dependence of the dynamic loss angle δ is decreasing with ω (see Fig. 3): this behavior can be explained by the enhanced contribution of the elastic component at higher frequency with respect to the viscous one.

It has to be mentioned here that, in the selected operative conditions, the frequency dependence of the viscous and elastic components is a function of the amplitude of deformation ϕ , as illustrated in Figs 4 and 5.

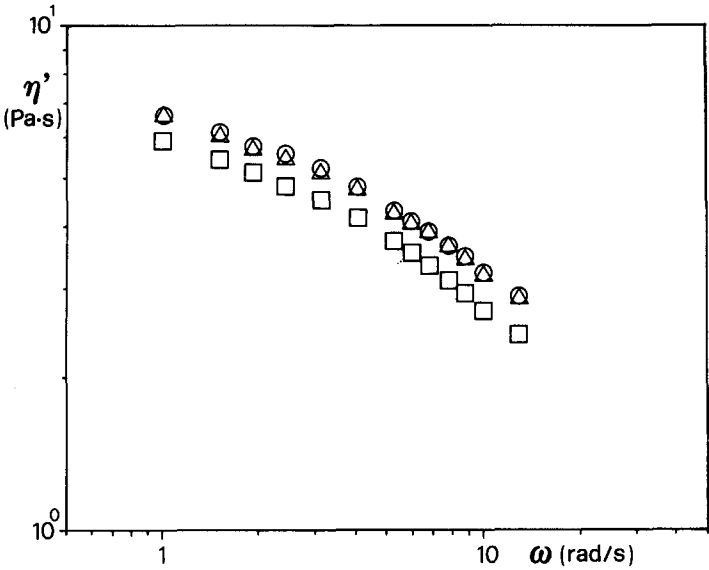


Fig. 4. Dynamic viscosity η' as a function of oscillation amplitude ϕ : \circ , $\phi = 0.0175$ rad; \triangle , $\phi = 0.0349$ rad; and \square , $\phi = 0.175$ rad.

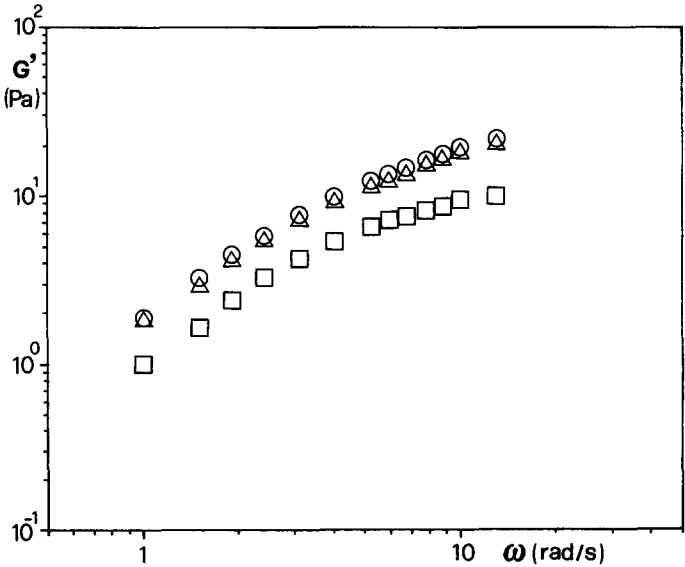


Fig. 5. Storage modulus G' as a function of oscillation amplitude ϕ : \circ , $\phi = 0.0175$ rad; \triangle , $\phi = 0.0349$ rad; and \square , $\phi = 0.175$ rad.

It appears from Fig. 4 that the η' values tend to converge at low ω ; the functional dependence of η' upon the oscillation frequency does not change by changing ϕ and only a shift towards lower values can be observed.

From the examples of shear viscosity η and dynamic viscosity η' data presented above it is evident that $\eta(\dot{\gamma})$ and $\eta'(\omega)$ are similar functions of their arguments: both these quantities approach the same limit value η_0 as $\dot{\gamma}$ and ω tend towards zero, and begin to decrease at comparable values of $\dot{\gamma}$ and ω . This empirical rule is known as the Cox-Merz rule (Cox & Merz, 1958), and an example of a 'Cox-Merz plot' is given in Fig. 6 for the HEG2 system. It has also been observed that, for all the samples considered, the convergence of $\eta(\dot{\gamma})$ and $\eta'(\omega)$ is more marked for lower values of the deformation amplitude ϕ .

As a confirmation of this empiricism it can be shown that the behavior of η' with ω can be described by means of an equation characterized by the same functional dependence of that employed for the fitting of $\eta(\dot{\gamma})$ data. Accordingly, the differences between the two functions are reduced to the differences in the characteristic times only.

By resorting to the two-parameter Cross model for $\eta(\dot{\gamma})$ and to an equivalent equation for $\eta'(\omega)$ — eqn (3):

$$\eta' = \frac{\eta_0}{1 + (\lambda' \omega)^{2/3}} \quad (3)$$

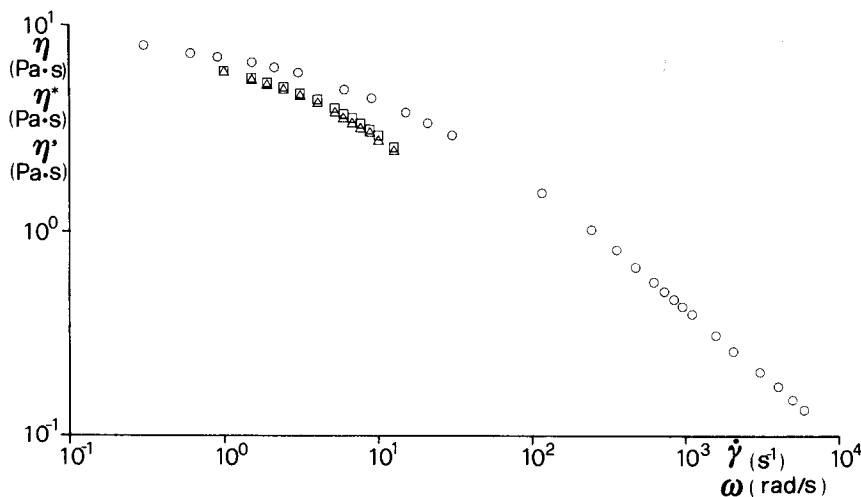


Fig. 6. Combined plot of steady shear viscosity η (\circ), complex viscosity η^* (\square) and dynamic viscosity η' (\triangle) plotted against shear rate/frequency ('Cox-Merz plot').

the characteristic parameters for the system HEG2 obtained from the fitting of the experimental data are the following: $\eta_0 = 9.23 \text{ Pa s}$; $\lambda = 0.0787 \text{ s}$; $\lambda' = 1.29 \text{ s}$; $n = 2/3$.

DEPENDENCE OF THE RHEOLOGICAL PROPERTIES ON POLYMER CONCENTRATION AND MOLECULAR PARAMETERS

Continuous shear tests

The effect of polymer concentration (C_p) on the shear-dependent behavior under continuous flow conditions of HEG aqueous solutions is reported in Fig. 7 for the HEG1, where the strong concentration dependence of $\eta(\dot{\gamma})$ at a given value of $\dot{\gamma}$ can be observed. This dependence is greater for lower values of the shear rate (see Fig. 8).

For those samples characterized by high values of C_p , the shear rate dependence of η is greater in the explored shear rate range. Moreover, as C_p is increased, the freedom of movement of the individual chains is

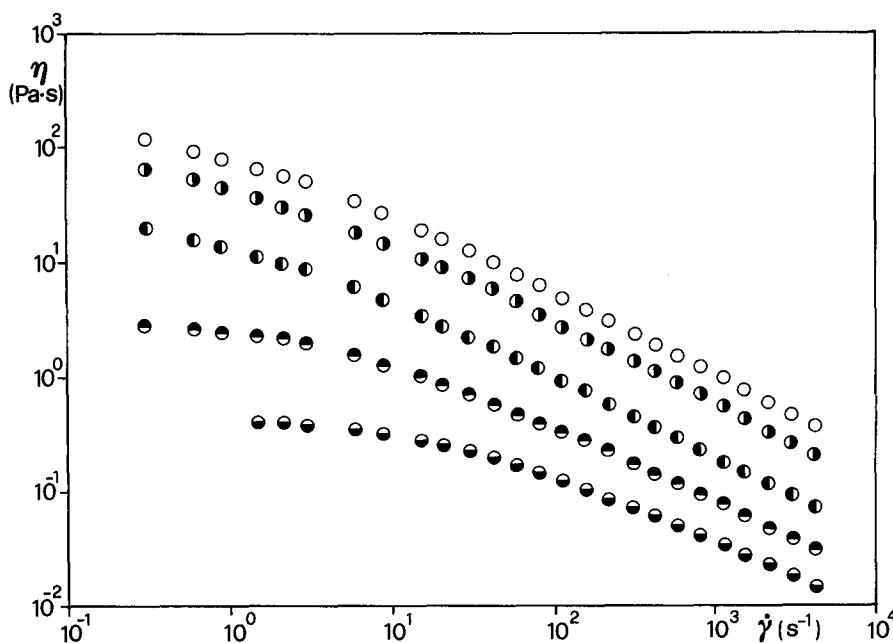


Fig. 7. Shear viscosity η versus shear rate $\dot{\gamma}$ for HEG1 at different polymer concentrations: ○, $C_p = 4.00\%$; ●, $C_p = 3.10\%$; ◐, $C_p = 2.32\%$; ⊗, $C_p = 1.50\%$; and ⊕, $C_p = 1.00\%$.

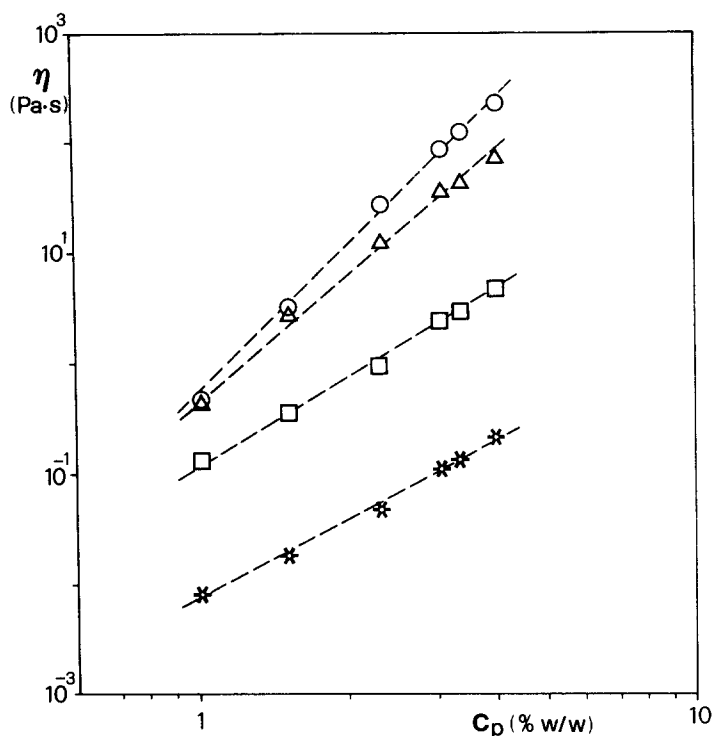


Fig. 8. Dependence of shear viscosity η on polymer concentration C_p at different shear rates for HEG1: \circ , $\dot{\gamma} = 10^{-2} \text{ s}^{-1}$; \triangle , $\dot{\gamma} = 10^0 \text{ s}^{-1}$; \square , $\dot{\gamma} = 10^2 \text{ s}^{-1}$; and \star , $\dot{\gamma} = 10^4 \text{ s}^{-1}$.

progressively restricted, with a consequent increase in time required to form new entanglements to replace those disrupted by the externally imposed deformation. Thus, as illustrated in Fig. 7, the shear rate at which Newtonian behavior is lost moves towards lower values with increasing polymer concentration.

As discussed before, all the viscosity-shear-rate data obtained for the HEG solutions can be fitted satisfactorily by means of the two-parameter Cross model, and the results obtained are reported in Figs 9 and 10.

The chance of setting $n = 2/3$ for all the three HEG series is strictly connected to the similar molecular weight distribution for all the HEG samples considered in this work (Cross, 1969).

The concentration dependence of η_0 is similar for all the HEG series (see Fig. 9), i.e. it is of the power-law type characteristic of concentrated polymer solutions:

$$\eta_0 = a \cdot C_p^\alpha$$

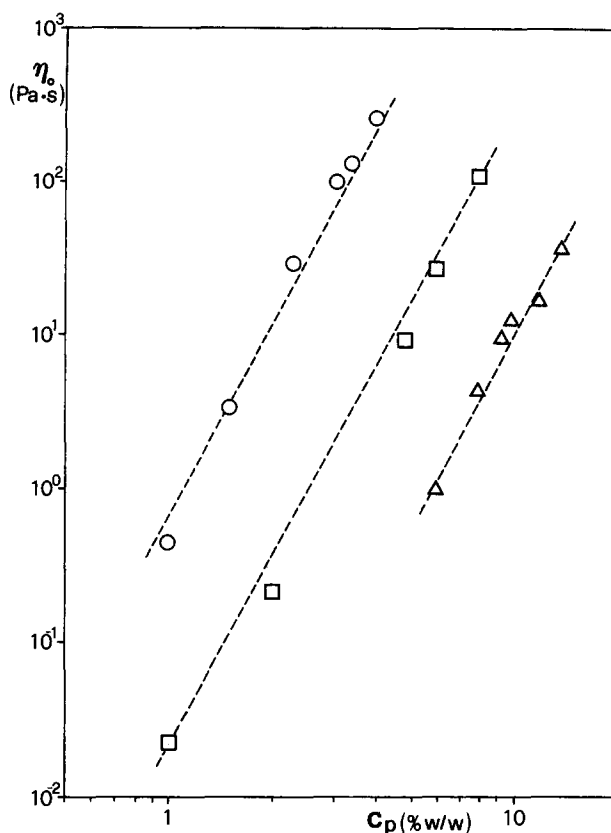


Fig. 9. Concentration dependence of zero-shear viscosity η_0 for the three HEG systems: ○, HEG1; □, HEG2; and △, HEG3.

The calculated value for the exponent α is 4.16; this result is in good agreement with previous works on disordered polysaccharides, even if the value of 4.16 is slightly higher than that predicted, for example by De Gennes (1979) for linear polymers interacting by purely topological entanglements: $\eta_0 \propto C_p^{3.75}$.

Analogous considerations can be drawn for the dependence of the characteristic time λ on polymer concentration (see Fig. 10); the value of the power-law exponent β in:

$$\lambda = a' \cdot C_p^\beta$$

calculated from the experimental data is 3.5.

As far as the significance of λ is concerned, Cross suggested identifying λ with a relaxation time, characterizing the viscoelasticity of the system (Cross, 1979). The inverse of λ , $\dot{\gamma}_c = 1/\lambda$, represents the shear

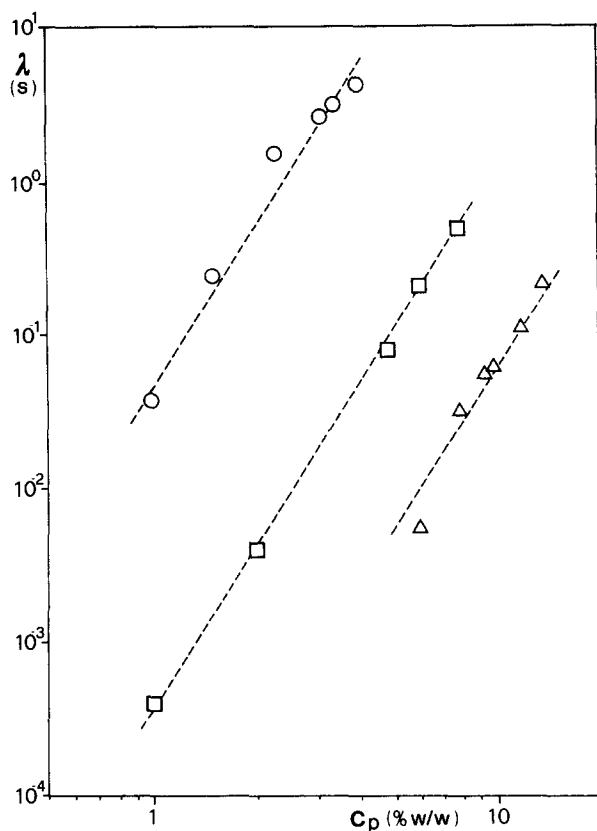


Fig. 10. Concentration dependence of characteristic time λ for the three HEG systems: ○, HEG1; □, HEG2; and △, HEG3.

rate at which the viscosity of the system is equal to $\eta_0/2$.

From the same data information can be obtained on the dependence of η_0 and λ on the molecular weight of the polymers. For concentrated polymer solutions, the dependence of the zero-shear viscosity on molecular weight is usually expressed by:

$$\eta_0 = bM^p$$

where p is close to 3.4–3.5 (Fox *et al.*, 1956). For the HEG series, a calculated value of 3.4 has been found for p , in agreement with theory.

Analogous dependence on molecular weight can be formulated for the characteristic time λ :

$$\lambda = bM^q$$

and the calculated value for q is 3.4.

Oscillatory flow tests

As it has been possible to remark in the previous section, the $\eta'(\omega)$ curves show profiles similar to those exhibited by the $\eta(\dot{\gamma})$ plots; the main differences can be found only in the values of the characteristic times λ and λ' . The ratio λ'/λ is practically independent of the molecular weight of the samples and is slightly increasing with C_p ; its values range from 8 up to 20.

As far as the elastic component is concerned, G' grows significantly by increasing ω , C_p and molecular weight. The variation of the dynamic loss angle δ with the oscillation frequency ω is reported in Fig. 11 for the sample HEG1 at different C_p . For low values of C_p and ω , the elastic component G' is negligible since δ is close to $\pi/2$.

The relevance of the elastic component G' as well as its variation with C_p and molecular weight are reported in Fig. 12, which shows the behavior of δ at a given value of ω .

EFFECT OF TEMPERATURE ON THE RHEOLOGICAL PARAMETERS

The temperature dependence of the shear viscosity $\eta(\dot{\gamma})$ can be described, in a narrow range of temperature, by the Andrade equation

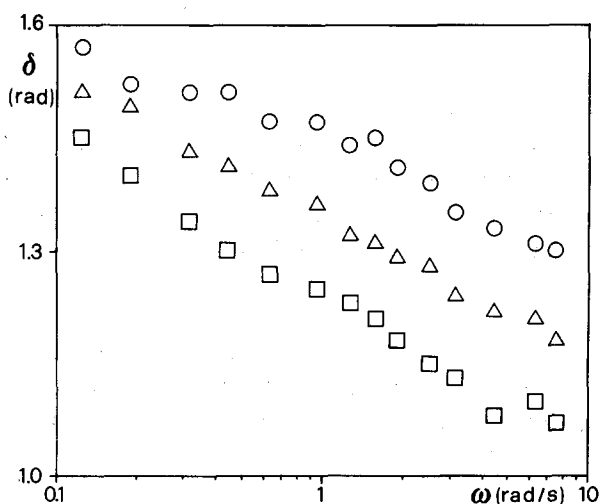


Fig. 11. Dynamic loss angle δ versus oscillation frequency ω for HEG1 at different polymer concentrations: ○, $C_p = 1.00\%$; Δ, $C_p = 1.50\%$; and □, $C_p = 2.32\%$.

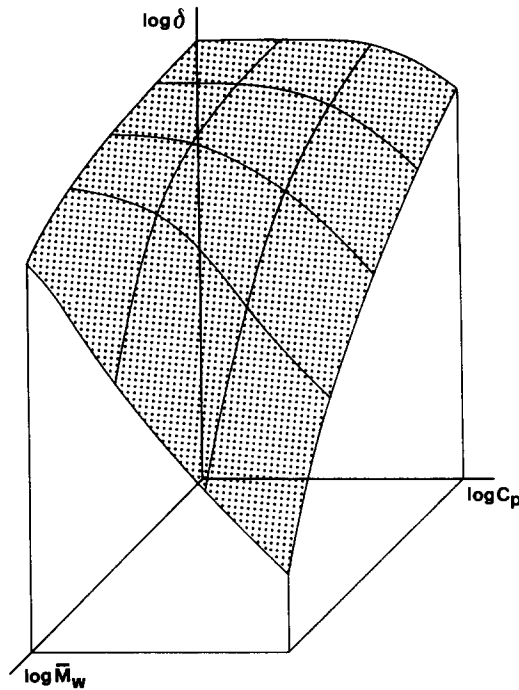


Fig. 12. Variation of the loss angle δ with polymer concentration C_p and molecular weight \bar{M}_w at $\omega = 0.314 \text{ rad s}^{-1}$.

(Andrade, 1930, 1934) — eqn (4):

$$\eta = A \exp\left(\frac{E_a}{RT}\right) \quad (4)$$

The pre-exponential factor A is the viscosity limit value for $T \rightarrow \infty$, if no other thermal processes were to occur at higher temperature; E_a is the activation energy for viscous flow. Both A and E_a are function of the applied shear rate.

Figure 13 shows the behavior of both A and E_a with $\dot{\gamma}$ for the system HEG2 ($C_p = 4.88\%$) taken as an example. The pre-exponential factor A decreases while decreasing $\dot{\gamma}$, with an asymptotic tendency towards a plateau value. This limit value can be calculated from the η_0 values of the Cross equation and, in this case, its numerical value is close to $2 \times 10^{-4} \text{ Pa s}$. On the other hand, the activation energy E_a increases by decreasing $\dot{\gamma}$. This behavior can be explained again in terms of entanglement formation in solution. In long-chain macromolecule solutions, where an entanglement network can be formed above a certain polymer con-

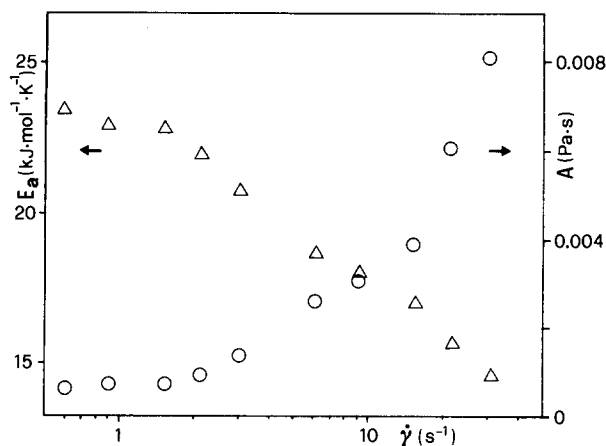


Fig. 13. Activation energy E_a and pre-exponential factor A plotted as function of shear rate $\dot{\gamma}$ for HEG2 ($C_p = 4.88\%$).

centration, the viscous flow is due to successive mobility of segments of the polymeric network from one position to another under the influence of thermal motion. In the Newtonian plateau zone, the entanglement density between polymer molecules is independent of the applied rate of deformation; consequently, the activation energy E_a is constant and its calculated value is $26.3 \text{ kJ mol}^{-1} \text{ K}^{-1}$. By increasing shear rate, the corresponding equilibrium entanglement density is lower; accordingly, a lower E_a is needed to promote viscous flow.

Analogous considerations can be drawn for the temperature dependence of the characteristic time λ ; even in this case, the Andrade equation can satisfactorily describe the variation of λ with temperature and the calculated activation energy values are comparable to those obtained for η_0 .

CONCLUSIONS

The flow properties of HEG aqueous solutions have been investigated, under continuous and oscillatory shear flow conditions, over a range of concentrations for three samples of different molecular weight.

The shear-dependent behavior of all the systems examined is markedly shear-thinning and can be satisfactorily described by means of Cross-type models. The dependence of the Cross parameters, η_0 and λ on concentration and molecular weight is that characteristic of concentrated solutions of polymers interacting by physical entanglements.

The temperature effect on the rheological properties of HEG aqueous systems has been described by the Andrade equation and discussed in terms of activation energy for viscous flow.

ACKNOWLEDGMENTS

We are very pleased to be able to thank Dr Carlo Nicora and Mr Giuseppe Molteni of the Fratelli Lamberti S.p.A., Albizzate, Italy, who kindly supplied the HEG samples.

REFERENCES

- Andrade, E. N. da C. (1930). *Nature*, **125**, 309.
Andrade, E. N. da C. (1934). *Phil. Mag.*, **17**, 497 and 698.
Carreau, P. J. (1968). PhD thesis. University of Wisconsin, Madison, WI.
Cox, W. P. & Merz, E. H. (1958). *J. Polym. Sci.*, **28**, 619.
Cross, M. M. (1965). *J. Colloid Sci.*, **20**, 417.
Cross, M. M. (1969). *J. Appl. Polym. Sci.*, **13**, 765.
Cross, M. M. (1979). *Rheol. Acta*, **18**, 609.
Dea, I. C. M. & Morrison, A. (1975). *Adv. Carbohydr. Chem. Biochem.*, **31**, 241.
De Gennes, P. G. (1979). *Nature (London)*, **282**, 367.
Ferry, J. D. (1980). *Viscoelastic Properties of Polymers*, 3rd edn, John Wiley & Sons, NY, USA.
Fox, T. G., Gratch, S. & Loshaek, S. (1956). In *Rheology: Theory and Applications*, Vol. 1, Chap. 12, ed. F. R. Eirich. Academic Press, New York, pp. 431-93.
Graessley, W. W. (1974). The entanglement concept in polymer rheology, *Adv. Polymer Sci.*, **16**, 1-179.
Johnson, J. F. & Porter, R. S. (1970). In *Progress in Polymer Science*, Vol. 2, Chap. 4, ed. A. D. Jenkins. Pergamon Press, New York, pp. 201-56.
Lapasin, R., Pricl, S., Graziosi, M. & Molteni, G. (1988). *Ind. Eng. Chem. Res.*, **27**, 1802.
Lee, Y.-C., Baaske, D. M. & Carter, J. E. (1983). *Anal. Chem.*, **55**, 334.
Morris, E. R., Cutler, A. N., Ross-Murphy, S. B. & Rees, D. A. (1981). *Carbohydr. Polymers*, **1**, 5.
Naik, S. C. (1980). In *Rheology*, Vol. 2, ed. G. Astarita, G. Marrucci & L. Nicolais. Plenum Press, New York and London.
Robinson, G., Ross-Murphy, S. B. & Morris, E. R. (1982). *Carbohydr. Res.*, **107**, 17.
Sharman, W. R., Richards, E. L. & Malcolm, G. N. (1978). *Biopolymers*, **17**, 2817.
Whistler, R. L. (ed.) (1973). *Industrial Gums*, 2nd edn. Academic Press, New York.